Vol. 602: 49–62, 2018
https://doi.org/10.3354/meps12692

MARINE ECOLOGY PROGRESS SERIES
Mar Ecol Prog Ser

Published August 23

Phytoplankton and bacterial dynamics on the Chukchi Sea Shelf during the spring–summer transition

Paige E. Connell[1], Christine Michel[2], Guillaume Meisterhans[2], Kevin R. Arrigo[3], David A. Caron[1,*]

[1]Department of Biological Sciences, University of Southern California, Los Angeles, CA 90089-0371, USA
[2]Fisheries and Oceans Canada, Winnipeg, Manitoba R3T 2N6, Canada
[3]Department of Environmental Earth System Science, Stanford University, Stanford, CA 94305, USA

ABSTRACT: Climate warming is exerting significant change on the physical properties of the Arctic Ocean, which in turn has marked consequences for the biology of the region. The Chukchi Sea is notable for its species richness as a consequence of a nutrient-rich shelf region that supports substantial primary production. However, little is known about the carbon transformations at the base of the food web in the Chukchi Sea, and in particular the relative amounts of primary production that are transferred directly to higher trophic levels or remineralized within the microbial loop. We measured microbial standing stocks (bacteria to microplankton), phytoplankton growth and mortality rates, and bacterial production and mortality rates at 10 stations in the Chukchi Sea and Bering Strait during the spring–summer transition. Our study revealed that protistan grazers consumed substantially more phytoplankton carbon than bacterial carbon. Phytoplankton growth rates were variable, but at times considerable (range: –0.06 to 0.71 d^{-1}), with protistan grazers consuming an average of 46% of the daily primary production. Heterotrophic protists exerted significant grazing pressure on phytoplankton despite low environmental temperatures. Bacterial production and mortality rates were low (generally <1 µg C l^{-1} d^{-1}) and at times in balance, but overall bacterial production exceeded mortality. This study improves our understanding of carbon cycling in the Chukchi Sea during the spring–summer transition, demonstrating a significant transfer of primary production to heterotrophic protists at that time of year.

KEY WORDS: Microbial food webs · Microzooplankton · Herbivory · Bacterivory · Phytoplankton growth · Bacterial production · Chukchi Sea

INTRODUCTION

The Chukchi Sea is a highly dynamic region of the Western Arctic Ocean that supports some of the highest primary production rates and photosynthetic biomass reported in oceanic environments (Springer & McRoy 1993, Arrigo et al. 2012, 2014). The delicate interplay of several water masses in the Arctic Ocean and the seasonal progression of the icescape defines the biogeochemistry, species composition, and overall productivity of the region. Nutrient-rich water enters the Chukchi Sea through the Bering Strait due to a sea-surface height differential (Weingartner et al. 2005). Additional nutrients are brought to the surface by convective mixing on the Chukchi Shelf, fueling a seasonal cycle of primary production as light availability increases during the spring–summer melt season. This broad, shallow continental shelf houses a rich benthic ecosystem that supports local marine bird and mammal populations (Grebmeier 2012).

The Arctic Ocean has experienced marked changes in recent decades which have impacted the Chukchi Sea. Documented changes include increased atmospheric and water temperatures, decreased ice thick-

*Corresponding author: dcaron@usc.edu

Publisher: Inter-Research · www.int-res.com

ness and extent, reduced persistence of multi-year ice, stronger wave activity resulting in enhanced coastal erosion, and predicted increases in precipitation and riverine input (Arrigo 2015, Dickinson et al. 2016). These changes have potentially profound implications for ecosystem function. Ice-free areas tend to have higher area-normalized carbon fixation rates than ice-covered areas (Brown & Arrigo 2013), thus a decrease in sea-ice extent may result in higher annual primary production (Arrigo & van Dijken 2015). Massive phytoplankton blooms have also been reported under the ice in recent years, challenging the paradigm that polar primary productivity is primarily confined to marginal ice zones and open waters (Arrigo et al. 2012, 2014, Lowry et al. 2014). A warming Arctic may also result in a tighter coupling between primary producers and herbivorous protists due to differential temperature effects on phototrophic and heterotrophic protists (Rose & Caron 2007), and increased encounter rates between predators and prey due to greater water column stratification (Behrenfeld & Boss 2014). Overall, climate change is expected to strengthen the 'microbial loop' in Arctic ecosystems, with a greater proportion of primary production providing dissolved organic matter for the growth of the heterotrophic bacterial assemblage (Kirchman et al. 2009b).

Protists are major sources of mortality for both phytoplankton and bacteria in marine environments (Sherr & Sherr 1994, 2002, Calbet & Landry 2004) and are known to be important consumers in the Arctic Ocean (Olson & Strom 2002, Sherr et al. 2009, 2013, Franzè & Lavrentyev 2014, 2017, Yang et al. 2014). Experiments that directly compare protistan grazing on phytoplankton and heterotrophic bacteria are rare, however, and to our knowledge no studies of this sort have been conducted in the Arctic Ocean. One study off East Antarctica indicated that, on average, roughly similar proportions of primary production and bacterial production were consumed by protists, although there was considerable variability in absolute values and their proportions (Pearce et al. 2010). In the Southern California Bight off the southwestern USA, phytoplankton were the dominant prey source for protistan grazers nearshore where nutrient concentrations were replete, yet roughly equal proportions of phytoplankton and bacterial carbon were removed at offshore locations (Connell et al. 2017). Off coastal Newfoundland, phytoplankton >0.7 µm were the primary prey source for protistan grazers during the spring, while heterotrophic bacteria and picophytoplankton were the primary prey source during the winter and summer seasons (Putland 2000). These results indicate shifting contributions of protists to top-down control of phytoplankton and bacterial assemblages, and a poor understanding of the relative contributions of these prey assemblages to the diets of protists in the ocean.

We characterized microbial food web dynamics in the Chukchi Sea during the spring–summer transition. Microbial abundances (bacteria to microzooplankton), phytoplankton growth and mortality rates, and bacterial production and mortality rates were measured during May and June 2014 on the Chukchi Shelf and in the Bering Strait. Measurements were made as part of the Study of Under-ice Blooms In the Chukchi Ecosystem (SUBICE) program, which sought to characterize the spatial distribution of under-ice phytoplankton blooms on the Chukchi Shelf and the physical, chemical, and biological mechanisms that control them. Phytoplankton growth and mortality rates demonstrated high variability throughout the region. Bacterial production and grazer-mediated mortality were comparable at 6 of 10 study sites while production exceeded mortality at 4 sites. Overall, phytoplankton were the primary food source for protistan grazers during the spring–summer transition in the Chukchi Sea, as substantially more phytoplankton carbon was consumed than bacterial carbon.

MATERIALS AND METHODS

Study site and environmental characterization

Microbial community composition and rate processes were measured from 16 May to 17 June 2014 as part of the SUBICE expedition. Sampling was conducted at 10 stations in the Pacific Sector of the Arctic Ocean aboard the R/V 'USCG Healy': 9 on the Chukchi Shelf and 1 in the Bering Strait (Fig. 1). Station numbers were kept consistent with the original numbering scheme from the SUBICE expedition and thus are nonconsecutive (total of 209 station numbers designated on the cruise).

Water was collected using the 'Healy's' 12-position, 30 l Niskin bottle system mounted on a CTD rosette. The research vessel was anchored in extant leads to enable CTD sampling of the water column despite the heavy ice cover present at most stations. A subsurface chlorophyll (chl *a*) maximum, visualized using real-time fluorescence data from the CTD downcast, was only detectable at 3 stations (29, 132, and 209). Water was collected from the surface (mean = 2.6 m) or at the subsurface chl *a* maximum (Stn 29; 10 m) on the CTD upcast. Seawater for com-

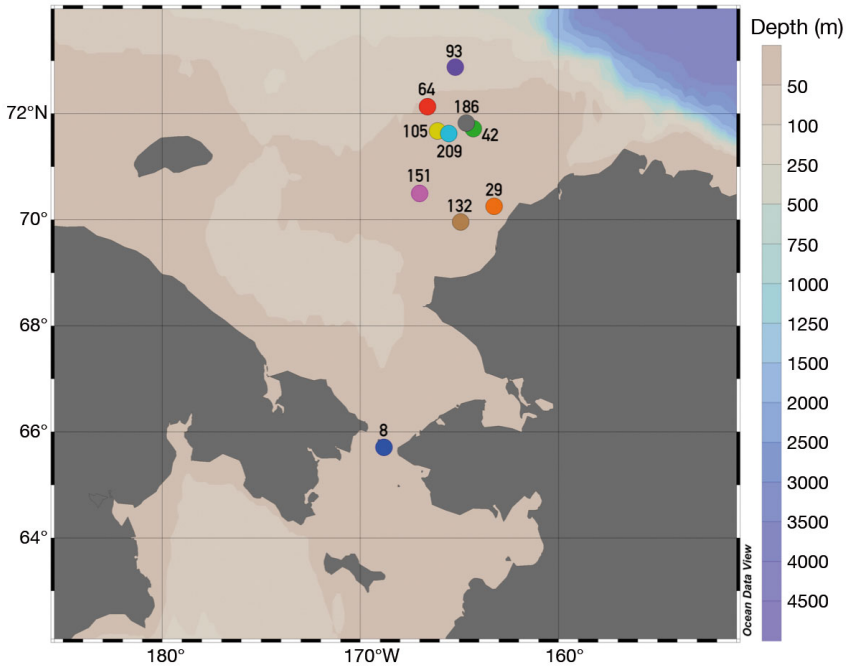

Fig. 1. Study location in the Chukchi Sea, Pacific Arctic Ocean, with bathymetry lines (color bar). Samples for microbial community composition and trophic activities were taken from 1 station in the Bering Strait (Stn 8) and 9 stations on the Chukchi Shelf. Station numbers follow the Study of Under-ice Blooms In the Chukchi Ecosystem (SUBICE) expedition site designations

munity composition and incubation experiments was transferred from the Niskin bottles into acid-rinsed (5% HCl), 23 l polycarbonate carboys with care taken to minimize bubbling that can damage delicate microzooplankton. Carboys were then transported to a low-light (~10 µmol photons m^{-2} s^{-1}), 0°C temperature-controlled room for experimental set-up and sampling. Water used to determine bacterial production rates was collected directly from the Niskin bottles into 20 ml scintillation vials.

Temperature and salinity were measured using dual temperature and conductivity sensors (SBE3/SBE4; Sea-Bird Electronics) on the CTD rosette, with the data quality-controlled post-cruise. Satellite sea ice concentrations were extracted for each station using SSM/I imagery at 25 km resolution as described in Arrigo & van Dijken (2015). Minimum distance (km) of each station from the shore was calculated to assess the potential impact of terrigenous input on microbial standing stocks and rate processes. Spearman's rank order correlation analysis with Bonferroni correction was conducted to determine significant relationships among all biological parameters (microbial abundances, phytoplankton growth rates, phytoplankton mortality rates, bacterial production rates, bacterial mortality rates), and all environmental parameters. Correlations between biological and environmental parameters were conducted on a per-volume basis.

Community composition and biomass

Picoplankton abundances (prokaryotic and eukaryotic cells, 0.2 to 2.0 µm in size) were determined for each station from triplicate samples collected at the beginning of the dilution experiments. Sample water was pre-filtered through 20 µm Nitex mesh, preserved with 1% formalin (final concentration), flash-frozen in liquid nitrogen, and stored at −80°C until flow cytometric analysis using a FACSCalibur flow cytometer (Becton Dickinson). Abundances of phototrophic picoeukaryotes were enumerated and distinguished from other picophytoplankton populations using the autofluorescence of the photosynthetic pigments and forward scatter. Phycoerythrin-containing cells consistent with *Synechococcus* were detected at some stations, which is in accordance with previous reports of *Synechococcus* in the region (Cottrell & Kirchman 2009, Laney & Sosik 2014). However, abundances were too low to reliably measure via flow cytometry and thus *Synechococcus* was not included in our analyses. Abundances of heterotrophic bacteria (*Bacteria* + *Archaea*, although we considered *Archaea* to be minor contributors to prokaryotic abundances in our samples, as observed in Wells & Deming 2003 and Garneau et al. 2006) were measured by flow cytometry using a standard SYTO13 (S7575; ThermoFisher Scientific) staining procedure (del Giorgio et al. 1996).

Abundances of nanoplankton (microbial eukaryotes, 2 to 20 µm in size) were determined for each station from formalin-preserved samples collected at the beginning of the dilution experiments (1% final conc.). Slides for microscopy were prepared using 30 ml aliquots of the preserved seawater filtered down to ~1 ml onto 25 mm diameter, 0.2 µm blackened polycarbonate filters, and stained with 50 µl of a 1 mg ml^{-1} working solution of 4′,6′-diamidino-2-phenylindole (DAPI; D9542; Sigma-Aldrich). Samples were then filtered down, rinsed with deionized water, and filters were placed onto glass slides with a

drop of immersion oil and a sealed coverslip. Slides were prepared in triplicate for each station and stored at –20°C until analysis by epifluorescence microscopy at 1000× magnification. Phototrophic (possibly mixotrophic) and heterotrophic nanoplankton were differentiated by the presence or absence of chlorophyll autofluorescence when viewed under blue-light excitation.

Abundances of microplankton (microbial eukaryotes, 20 to 200 µm in size) were determined using inverted light microscopy. Formalin-preserved samples (1% final conc.) of seawater were collected at the beginning of the dilution experiments for each station. Aliquots (25 to 250 ml) of the preserved seawater were settled for 24 to 48 h in Utermöhl chambers and the abundances of diatoms, dinoflagellates, and ciliates were enumerated at 400× magnification (Utermöhl 1958).

Cell abundances were converted to carbon biomasses using carbon conversion factors obtained from the literature for appropriate Arctic ecosystems. Bacterial abundance was converted to carbon biomass using a conversion factor of 15.2 fg C cell^{-1} (Ortega-Retuerta et al. 2012). The abundances of the other microbial groups were converted to carbon biomasses by applying the conversion factors used in Terrado et al. (2008) for the Beaufort Sea: 0.49 pg C cell^{-1} for phototrophic picoeukaryotes, 5.8 pg C cell^{-1} for phototrophic/mixotrophic and heterotrophic nanoplankton, 242 pg C cell^{-1} for ciliates and dinoflagellates, and 113 pg C cell^{-1} for diatoms. Dinoflagellates can have a diverse array of nutritional modes (phototrophic, mixotrophic, heterotrophic; Taylor et al. 2008) that were not distinguished in this study. Dinoflagellate biomass was thus split evenly between phototrophic and heterotrophic nutritional modes when calculating total phytoplankton biomass or total heterotrophic grazer biomass. The choice of these carbon conversion factors gave an average C:chl *a* ratio of 41 for our study, which falls within the range of commonly observed C:chl *a* factors for the Western Arctic Ocean (i.e. 30 used by Sherr et al. 2009; 88.5 used in Ortega-Retuerta et al. 2014).

Size-fractionated chl *a* was also measured at each station. Four size fractions (unfiltered seawater, <200, <20, and <5 µm filtrate) were prepared by sequentially filtering water collected at the beginning of the experiments through in-line filters equipped with 200, 20, and 5 µm Nitex mesh, and collecting the filtrate in darkened, polycarbonate bottles. Sample water (100 to 250 ml) was then filtered in triplicate onto 25 mm GF/F filters (nominal pore size 0.7 µm). Filters were extracted in 5 ml of 90% acetone for 24 h, in the dark, at 0°C. Samples were processed using a calibrated Turner 10-AU fluorometer (Turner Designs) and the acidification method (Holm-Hansen et al. 1965, Arar & Collins 1997).

Protistan growth and herbivory by dilution experiments

The growth and grazing mortality rates of the total phytoplankton community (using chl *a* as a proxy for phytoplankton biomass) and the phototrophic picoeukaryotes (using flow cytometry) were determined using a modified dilution method (Landry & Hassett 1982, Landry et al. 1995). The dilution method enables simultaneous measurement of the nutrient-enriched growth rates (μ_n), intrinsic (unenriched) growth rates (μ_0), and grazing mortality rates (m) of the phytoplankton community (as well as specific phytoplankton groups) through the sequential dilution of unfiltered seawater with 0.2 µm diluent prepared from the same seawater. A 5 point dilution series (100, 80, 60, 40, and 20% unfiltered seawater) was prepared in triplicate in acid-rinsed 1.2 l polycarbonate bottles at low light in a 0°C cold room. Nutrient stock (1 ml) was added to the bottles in the dilution series at a final concentration of 10 µM $NaNO_3$, 1 µM NH_4Cl, and 0.7 µM $NaP_2PO_4{\cdot}H_2O$ to prevent nutrient-limitation of phytoplankton growth (Landry et al. 1995). A treatment of unenriched, unfiltered seawater was also prepared in triplicate to enable the calculation of intrinsic phytoplankton growth rates (μ_0) and to assess the impact of nutrient addition on the phytoplankton assemblage. In addition, <200 µm filtrate was prepared using an acid-rinsed in-line filter equipped with 200 µm Nitex mesh and incubated in triplicate 1.2 l bottles without the addition of nutrients to determine the grazing impact of protistan grazers (nano- and microzooplankton) in the absence of mesozooplankton.

Bottles were transferred to an on-deck, flow-through incubator maintained at *in situ* temperatures and incubated for 24 to 72 h, depending on the initial chl *a* concentration (see Table S1 in the Supplement at www.int-res.com/articles/suppl/m602p049_supp.pdf). Neutral-density screening covered the bottles to mimic *in situ* light conditions (Table S1), as photoadaptation of the phytoplankton can result in erroneous estimations of µ when using chl *a* as a proxy of phytoplankton biomass. The extent of photoadaptation experienced by the phytoplankton during the

incubation period was measured using fast repetition rate fluorometry (FRRf) to monitor changes in the maximum efficiency of photosystem II (F_v/F_m) (Kolber et al. 1998) (for details, see text in the Supplement).

Chl *a* concentrations and phototrophic picoeukaryote abundances were measured in all dilution experiments. Triplicate chl *a* samples and triplicate flow cytometry samples were analyzed from the initial unfiltered seawater, <200 µm filtrate, and <0.2 µm filtrate. Duplicate chl *a* samples and a single flow cytometry sample were analyzed from each of the triplicate bottles within each treatment at the end of the experiment.

Model I linear regressions of plots of the apparent growth rate (*y*-axis) against the dilution factor (*x*-axis) were used to calculate μ_n (*y*-intercept of the regression) and *m* (slope of the regression) of the total phytoplankton and phototrophic picoeukaryotic assemblages (Landry & Hassett 1982). μ_0 of these assemblages were determined from growth in the unenriched treatment and the mortality rate (Landry et al. 1995). Comparisons of the rates derived from these regression analyses were performed using *t*-tests. Non-linear dilution curves indicative of grazing saturation were detected for the total phytoplankton community at Stns 29 and 186; for these stations, regressions to determine µ and *m* were obtained from the 3 highest dilution levels (Gallegos 1989). Grazing saturation was not observed for the phototrophic picoeukaryotes. Differences in the phytoplankton growth rates between the μ_n and μ_0 treatments, as well as differences in apparent growth rate between the unfiltered seawater and <200 µm filtrate unenriched treatments were assessed using Welch's 2-sample *t*-tests.

The percentage of primary production removed daily was calculated as m:μ_0 ratio × 100 (Calbet & Landry 2004). The daily percent standing stock removal of the total phytoplankton (chl *a*-based) and phototrophic picoeukaryotic assemblages (%SS) was determined according to the following equations:

$$\%SS = G \times (100 / C_0) \quad (1)$$

$$G = m \times C_m \quad (2)$$

$$C_m = C_0[e^{(\mu 0 - m)t} - 1] / (\mu_0 - m)t \quad (3)$$

where μ_0 and *m* are the respective rates per day, *t* is length of the incubation (d), C_0 is the initial chl *a* concentration (or phototrophic picoeukaryote abundance), C_m is the mean chl *a* concentration (or phototrophic picoeukaryote abundance) during the incubation, and *G* is the grazing impact of the consumers (Calbet & Landry 2004).

Bacterial production and bacterivory rates

Bacterial production using radiolabeled leucine

Bacterial production rates were measured in triplicate at each station based on the incorporation rates of ^{3}H-leucine according to the centrifugation protocol (Smith & Azam 1992), as detailed in the text in the Supplement. Data were converted from pmol Leu l^{-1} h^{-1} to units of bacterial carbon using a conversion factor of 1.5 kg C mol^{-1} of ^{3}H-leucine, which has previously been used in the Chukchi Sea and Western Arctic Ocean (Kirchman et al. 2009a, Ortega-Retuerta et al. 2014).

Bacterial grazing mortality by fluorescently labeled bacteria disappearance

Bacterial grazing mortality was determined by following the disappearance of fluorescently labeled bacteria (FLB) in natural seawater samples. FLB were prepared from a culture of *Dokdonia donghaensis* as detailed in the text in the Supplement. FLB disappearance experiments consisted of 2 sets of triplicate 1.2 l polycarbonate bottles, one containing unfiltered seawater (to assess FLB disappearance attributable to grazing) and the other containing 0.2 µm filtrate (to serve as a control for non-grazing losses of FLB in the bottles). FLB aliquots were vigorously vortexed and passed through a 3.0 µm polycarbonate filter to remove clumps before their addition to experimental bottles at ~20% of the natural bacterial abundance (mean T_0 FLB abundance = 1.07×10^5 FLB ml^{-1}, mean T_0 natural bacterial abundance = 5.78×10^5 cells ml^{-1}, which are the abundances at the beginning of the incubation). FLB disappearance experiments were incubated alongside the dilution experiments in the on-deck, flow-through incubator and were exposed to the same incubation temperatures, light conditions, and incubation lengths detailed in the 'Protistan growth and herbivory by dilution experiments' section. Changes in the FLB abundances in the unfiltered seawater treatment were used to calculate bacterial removal due to grazing (taking into account the non-grazing changes in abundances measured in the control treatment). Samples for flow cytometry were collected at the beginning of each experiment immediately after the addition of FLB, and at the end of each experiment. Samples were preserved in 1% formalin (final conc.), flash-frozen in liquid nitrogen, and stored at –80°C until analysis by flow cytometry.

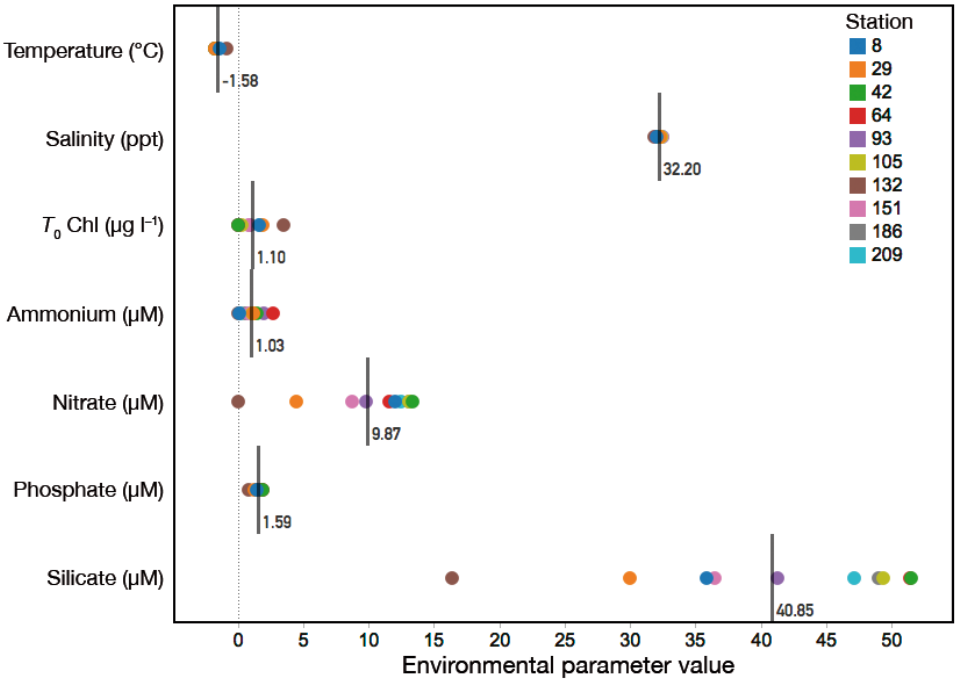

Fig. 2. Mean (vertical black bars) and station-specific (color-coded symbols) values for environmental parameters measured during the study. Environmental parameters include temperature (°C), salinity (PSS-78), chl *a* at the beginning of the incubation (T_0 chl *a*; µg l^{-1}), ammonium (µM), nitrate (µM), phosphate (µM), and silicate (µM)

Bacterial mortality rate (g; d^{-1}) was calculated according to the following equation,

$$g = \ln(F_t / F_0) \times (-1 / t) \quad (4)$$

where F_0 is the number of FLB added at the beginning of the incubation and F_t is the number of FLB remaining at the end of the incubation (Marrasé et al. 1992). Bacterial consumption rate (µg bacterial C consumed ml^{-1} d^{-1}) was calculated by multiplying the bacterial grazing mortality rate (d^{-1}) by the bacterial standing stock (µg C ml^{-1}) at each station.

RESULTS

Environmental conditions during the spring–summer transition

Water temperatures ranged from −1.74 to −0.84°C (mean = −1.58°C) throughout the study region, and salinities ranged from 31.90 to 32.49 (mean = 32.2) (Fig. 2). The water column was isothermal at the majority of stations (n = 9). Water column depths ranged from 32 to 63 m (mean = 45.7 m), and ice cover from 46 to 100%, with more than 90% ice coverage at 7 of the 10 stations (see Fig. S1 in the Supplement). A late season snowfall (between 4 and 8 June) delayed the onset of the melt season compared to previous years, reducing light availability below the ice. Macronutrients were replete at most stations during the cruise (Fig. 2). Dissolved N:P ratios were low (mean = 6), and initial chl *a* concentrations among the experiments ranged from 0.04 to 3.49 µg l^{-1} (mean = 1.10 µg l^{-1}) and were negatively correlated with ammonium ($\rho = -0.78$, $p < 0.01$), phosphate ($\rho = -0.81$, $p < 0.01$), and silicate ($\rho = -0.83$, $p < 0.01$) concentrations. Nitrate drawdown was apparent at Stns 29 and 132 (Fig. 2). Chl *a* concentration was not correlated with the percentage of ice cover at each station.

Abundances and standing stocks of the microbial assemblage

The standing stock of carbon for the microbial communities varied greatly by station (range = 7.29 to 347 µg C l^{-1}; Fig. 3a), with differences largely driven by variability in diatom abundances between stations (coefficient of variation of 151%; Fig. 3a). Total microbial standing stock was negatively correlated with distance from shore ($\rho = -0.81$, $p < 0.01$), but was not correlated with the percentage of ice cover at each station. The highest microbial standing stocks observed during our study were located off Point Lay, Alaska, at Stns 132 and 29; the lowest were recorded at the most northerly stations (Stns 64 and 93; Fig. 1).

Heterotrophic bacterial abundances ranged from 1.8×10^5 to 1.1×10^6 cells ml^{-1}, which corresponds to bacterial biomass values of 2.68 to 16.3 µg C l^{-1}

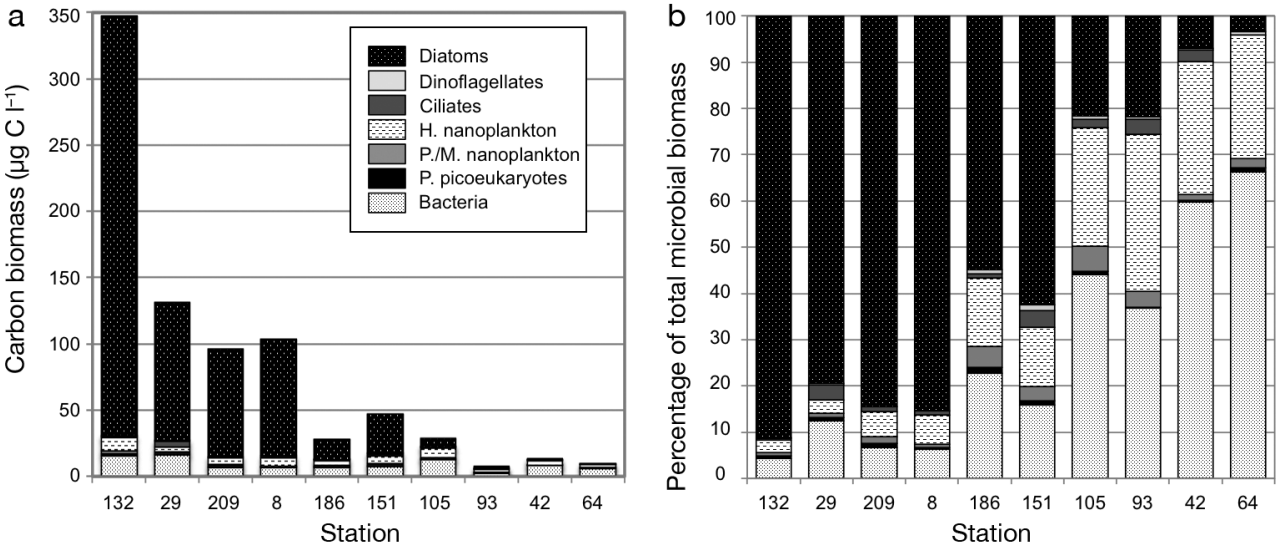

Fig. 3. (a) Absolute (µg C l^{-1}) and (b) relative (%) contributions of the microbial assemblages to living carbon biomass at each station. Stations are arranged by descending chl *a* concentration (left to right). Microbial assemblages measured include bacteria, phototrophic (P.) picoeukaryotes, phototrophic/mixotrophic (P./M.) nanoplankton, heterotrophic (H.) nanoplankton, ciliates (loricate + aloricate), dinoflagellates, and diatoms

(Fig. 3a). Bacteria were generally <20% of the total microbial biomass except at the low chl *a* stations where they constituted more than half of the microbial community biomass (Fig. 3b).

Phytoplankton biomass and composition varied greatly between sites. Diatom biomass ranged from 0.31 to 316 µg C l^{-1}, constituting between 4 and 93% of the total microbial standing stocks among the stations (Fig. 3). Phototrophic (including mixotrophic) nanoplankton and picoeukaryote standing stocks were smaller and more consistent between sites, ranging from 0.19 to 2.43 and 0.02 to 1.57 µg C l^{-1}, respectively. Eukaryotic phytoplankton <20 µm in size never exceeded ~5% of the total microbial biomass (Fig. 3b). The predominance of large phytoplankton during our study was also highlighted by the size-fractionated chl *a* concentrations. Phytoplankton >20 µm (predominantly diatoms) constituted ≥50% of the total chl *a* at 9 of 10 stations (Fig. 4a). A total of 23 distinct diatom genera were observed in the study region (Fig. 4b). *Fragillariopsis* and *Navicula septentrionalis*, which are morphologically similar and were grouped to reduce misidentification, were the most abundant diatoms at 9 of 10 stations. *Melosira varians* was also abundant at half of the stations, especially those with high chl *a* concentrations. Diatom abundances were negatively correlated with ammonium, phosphate, and silicate concentrations (see Table S2).

The total biomass of heterotrophic grazers ranged from 2.55 to 11.1 µg C l^{-1} and constituted between 6.4 and 37% of total microbial community standing stocks (Fig. 3). Heterotrophic nanoplankton biomass (range = 2.47 to 9.78 µg C l^{-1}) exceeded microzooplankton biomass (ciliates and dinoflagellates; range = 0.08 to 4.79 µg C l^{-1}) at all stations except Stn 29, where ciliate biomass was maximum (4.26 µg C l^{-1}). Total dinoflagellate biomass consistently fell below 1 µg C l^{-1} (assuming half the cells were phototrophic, heterotrophic dinoflagellate biomass was <0.5 µg C l^{-1}).

Neither heterotrophic nanoplankton biomass nor dinoflagellate biomass were correlated with prey biomasses. However, ciliate biomass was positively correlated with bacterial (ρ = 0.65), phototrophic picoeukaryote (ρ = 0.70), and diatom biomass (ρ = 0.78) (all $p < 0.05$).

Microbial rate processes

Phytoplankton growth and mortality rates

Unenriched μ_0 of the total phytoplankton community (based on chl *a*) ranged from –0.06 to 0.71 d^{-1} (mean = 0.47 d^{-1}; Table 1). F_v/F_m values were relatively high and unwavering throughout the incubation period in all experiments, indicating that phytoplankton growth rates were not impacted by light-stress (Table S1). Nutrient addition significantly enhanced phytoplankton growth rates only at Stn 132 (Table S3). Phytoplankton growth rates (both μ_0 and μ_n) were not correlated with any of the environmental factors (Table S2).

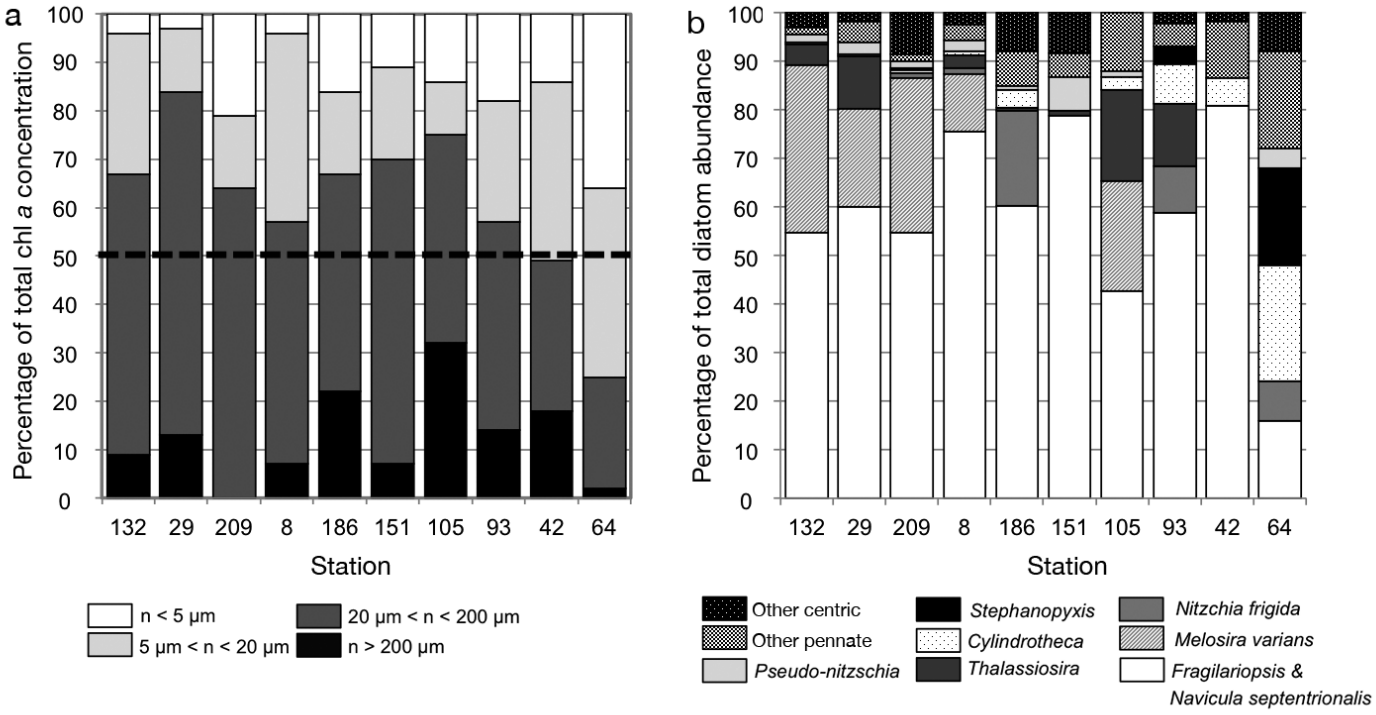

Fig. 4. Phytoplankton community composition based on (a) size-fractionated chl *a*, represented as percentage of the total chl *a* concentration detected in each size fraction, and (b) diatom group abundances, represented as the percentage of the total diatom community constituted by each group. Stations are arranged by descending chl *a* concentration (left to right)

Mortality rates of the total phytoplankton community ranged from undetectable to 0.73 d^{-1} (mean = 0.25 d^{-1}), and accounted for the removal of approximately half of the daily primary production (mean = 46% d^{-1}; excluding Stn 132 where values were ≫100%) and approximately one-third of the daily phytoplankton standing stock (mean = 30% d^{-1}) (Table 1). Phytoplankton mortality rates were comparable to phytoplankton unenriched growth rates at only 2 of the 10 stations (Fig. 5a). Grazers removed >100% of the daily primary production at the stations with the highest chl *a* concentrations (Stns 29 and

Table 1. Initial chlorophyll *a* (chl *a*) concentrations (µg l^{-1}), temperatures (°C), grazing mortality rates (m), nutrient-enriched growth rates (μ_n), intrinsic (unenriched) growth rates (μ_0), and the percentage of daily primary production (%PP) or standing stock (%SS) removed for the total phytoplankton community (based on chl *a*) and the phototrophic picoeukaryotes (based on flow cytometry) for each station sampled during the study period. The m and μ_n rates were calculated using model I linear regressions; μ_0 were adjusted from μ_n values. Mean values (±SD) of each parameter are contained in the bottom row. Asterisks indicate significance of the model I linear regression at the denoted p-value (*p < 0.05, **p < 0.01, ns: non-significant); ns values were included as 'zeros' when calculating mean mortality rates for each assemblage

Station	Date	T_0 chl *a* (µg l^{-1})	Temp (°C)	Total phytoplankton (chl *a*) m (d^{-1})	μ_n (d^{-1})	μ_0 (d^{-1})	%PP	%SS	Phototrophic picoeukaryotes m (d^{-1})	μ_n (d^{-1})	μ_0 (d^{-1})	%PP	%SS
8	16-May-14	1.67	−1.34	0.32*	0.44	0.71	45	39	ns	0.42	0.62	0	0.0
29	20-May-14	1.91	−1.74	0.73**	0.33	0.70	104	72	ns	−0.35	−0.41	0	0.0
42	23-May-14	0.04	−1.71	0.1**	0.33	0.32	31	14	ns	−0.05	0.06	0	0.0
64	27-May-14	0.04	−1.69	0.26**	0.44	0.50	52	38	ns	0.12	0.36	119	39
93	01-June-14	0.06	−1.72	ns	0.54	0.57	0.0	0.0	0.66**	0.63	0.92	72	2.2
105	04-June-14	0.34	−1.73	0.18**	0.30	0.26	69	20	ns	0.06	0.09	0	0.0
132	08-June-14	3.49	−0.84	0.19*	0.20	−0.06	≫100	17	ns	0.21	0.51	0	0.0
151	10-June-14	0.85	−1.72	0.31**	0.55	0.67	46	46	0.36**	0.20	0.31	116	34
186	14-June-14	0.90	−1.69	0.41*	0.42	0.61	67	51	0.55*	0.17	0.17	324	39
209	17-June-14	1.71	−1.59	ns	0.40	0.45	0.0	0.0	ns	0.10	0.16	0	0.0
	Mean (±SD)	1.10 (±1.11)	−1.5 (±0.28)	0.258 (±0.22)	0.40 (±0.11)	0.47 (±0.24)	46 (±33)	30 (±23)	0.20 (±0.27)	0.15 (±0.26)	0.28 (±0.36)	63 (±104)	11 (±18)

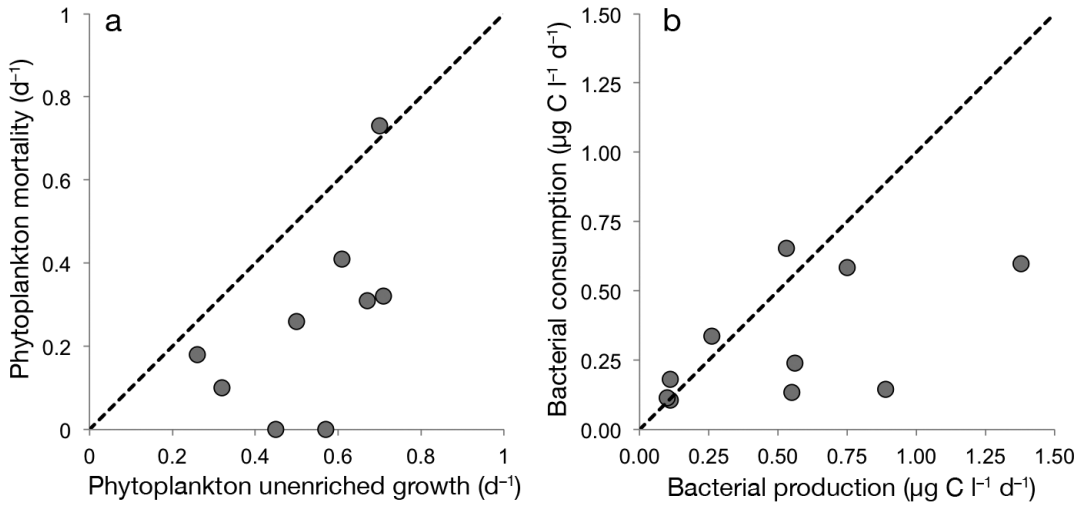

Fig. 5. Comparisons of growth and mortality for the phytoplankton and bacterial assemblages. (a) Phytoplankton unenriched growth rate (d^{-1}) vs. phytoplankton mortality rate (d^{-1}), and (b) bacterial production rate (µg C l^{-1} d^{-1}) vs. bacterial consumption rate (µg C l^{-1} d^{-1}) at the 10 stations sampled. Black dashed line represents a 1:1 relationship

132; Table 1), which were both located closest to land near Point Lay, Alaska. Interestingly, the intrinsic phytoplankton growth rate was high at Stn 29 (0.70 d^{-1}), which showed moderate drawdown of nitrate and silicate concentrations, but negligible at Stn 132 (–0.06 d^{-1}), which had the lowest nitrate concentration and highest chl *a* value (Table 1, Fig. 2). Phytoplankton mortality rates were undetectable (regressions were non-significant) at 2 stations (93 and 209). Phytoplankton mortality rate was not correlated with any of the environmental factors (Table S2).

Intrinsic growth rates of the phototrophic picoeukaryotes were highly variable, ranging from –0.41 to 0.92 d^{-1} (mean = 0.28 d^{-1}; Table 1). Nutrient addition did not significantly affect the growth rates of the phototrophic picoeukaryotes in any of the experiments conducted (Table S3). Mortality rates of the phototrophic picoeukaryotes averaged 0.20 d^{-1}, but were non-significant at 7 stations (Table 1). The 3 stations yielding detectable phototrophic picoeukaryotic mortality rates averaged 0.52 d^{-1} (0.36 to 0.66 d^{-1}). Grazers removed between 72 and 324% of the daily phototrophic picoeukaryotic production and between 2.2 and 39% of the phototrophic standing stock per day at those stations.

Generally, removing metazoan grazers did not impact the apparent growth rates of the phytoplankton. This result is not unexpected given the time of year (microzooplankton would be expected to play a larger role as summer progresses). However, apparent growth rates in the <200 µm, unenriched treatment (without metazoan grazers) were significantly higher than apparent growth rates in the unfiltered, unenriched treatment (100%) (with metazoan grazers) for the total phytoplankton community at Stn 42 and for the phototrophic picoeukaryotes at Stns 186 and 209 (Table S3). Ciliate biomass and phytoplankton mortality rate were positively correlated ($\rho = 0.56$, $p < 0.05$), but no significant relationship could be detected between dinoflagellate biomass or heterotrophic nanoplankton biomass and the mortality rates of the total phytoplankton community or the phototrophic picoeukaryotes.

Bacterial production and mortality rates

Bacterial production rates ranged from 0.10 to 1.38 µg C l^{-1} d^{-1} (mean = 0.52 µg C l^{-1} d^{-1}), which corresponds to bacterial growth rates of 0.01 to 0.12 d^{-1} (Table 2). Both bacterial standing stocks and rates of bacterial production were significantly higher at stations that were closer to the shore based on linear regressions of those variables against minimum distance from shore ($p < 0.05$). Bacterial production rate also correlated positively with chl *a* concentration (Table S2). Bacterial grazing mortality rates were low throughout the study, ranging from 0.01 to 0.11 d^{-1} (mean = 0.03 d^{-1}; Table 2), with the highest rate observed in the Bering Strait. These values corresponded to bacterial carbon consumption rates of 0.11 to 0.65 µg C l^{-1} d^{-1} (mean = 0.31 µg C l^{-1} d^{-1}). Bacterial mortality rate was not correlated with total heterotrophic grazer biomass or with the biomass of individual grazer groups.

Table 2. Rates of bacterial grazing mortality (m; d^{-1}), bacterial growth (μ; d^{-1}), bacterial carbon consumption by grazers (consumption; μg C l^{-1} d^{-1}), and bacterial production (production; μg C l^{-1} d^{-1}) at each station surveyed during our study. Bacterial grazing mortality rates were measured using the disappearance of fluorescently labeled bacteria, and bacterial production rates were measured using ^{3}H-leucine incubations. Bacterial carbon consumption rates and bacterial growth rates were then calculated from these measurements as detailed in the 'Materials and methods'

Station	m (d^{-1})	μ (d^{-1})	Consumption (μg C l^{-1} d^{-1})	Production (μg C l^{-1} d^{-1})
8	0.11	0.08	0.65	0.53
29	0.04	0.05	0.59	0.75
42	0.00	0.01	0.11	0.11
64	0.01	0.02	0.18	0.11
93	0.01	0.04	0.12	0.10
105	0.01	0.02	0.34	0.26
132	0.04	0.09	0.60	1.38
151	0.01	0.12	0.15	0.89
186	0.02	0.09	0.24	0.56
209	0.01	0.09	0.13	0.55
Mean ± SD	0.03 ± 0.03	0.06 ± 0.04	0.31 ± 0.22	0.52 ± 0.41

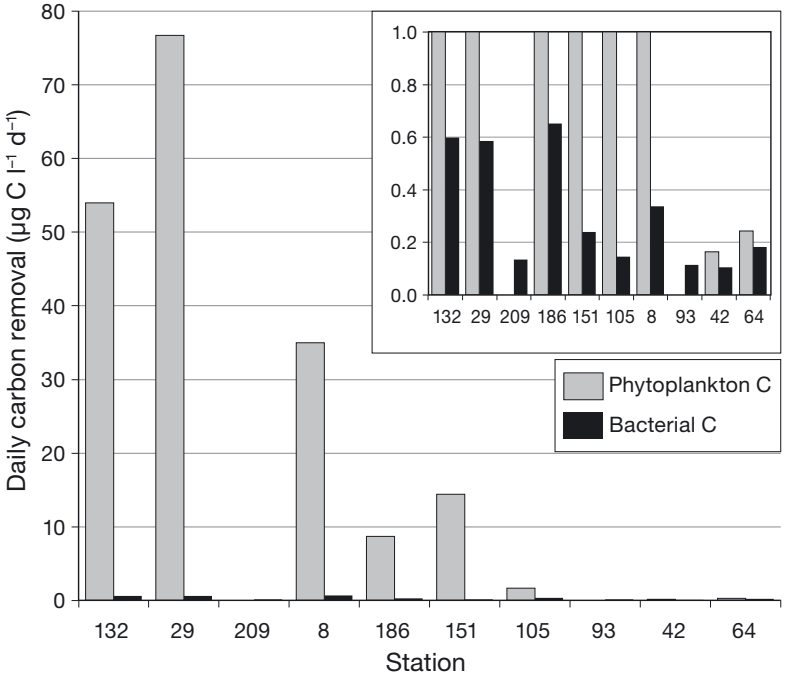

Fig. 6. Mean daily carbon removal (μg C l^{-1} d^{-1}) by protistan grazers from the phytoplankton (gray columns) and heterotrophic bacterial (black columns) assemblages at each station. Stations are arranged by descending chl *a* concentration (left to right). Insert depicts the same data on a different *y*-axis scale to provide visual clarity for low carbon removal values

Rates of carbon production by bacteria and bacterial carbon consumption by grazers were relatively balanced at 6 of 10 stations (mean = 0.31 vs. 0.33 for production and grazing, respectively, for those 6 stations; Table 2, Fig. 5b) but bacterial production rates clearly exceeded bacterial consumption rates at 4 stations (mean = 0.84 vs. 0.28, respectively for those 4 stations). Overall, protistan consumption of bacterial carbon (mean = 0.31 μg C l^{-1} d^{-1}) removed an average of 60% of the mean bacterial production, which was 0.52 μg C l^{-1} d^{-1}.

Carbon flow to higher trophic levels

Daily phytoplankton carbon removal by grazers was quite variable between sites, ranging from 0 to 76.7 μg C l^{-1} d^{-1} (mean = 19.1 μg C l^{-1} d^{-1}), while daily bacterial carbon removal by grazers was much more constant in comparison, ranging from 0.11 to 0.65 μg C l^{-1} d^{-1} (mean = 0.31 μg C l^{-1} d^{-1}). Substantially more phytoplankton carbon was consumed daily than bacterial carbon at most stations where phytoplankton grazing mortality rates could be detected (Fig. 6, Table 1). The average ratio of daily phytoplankton carbon consumption to bacterial carbon consumption was 62 during the study.

DISCUSSION

This study provides unique insight into microbial standing stocks and rate processes during the spring–summer transition in the Chukchi Sea, a season which has been historically under-sampled due to heavy ice cover. Phytoplankton μ_0 were highly variable (range of –0.06 to 0.71 d^{-1}; Table 1) across the shelf during this period. The mean μ_0 reported in our study (0.47 d^{-1}) was higher than other mean μ_0 reported for the Chukchi and Bering seas during the spring–summer transition (means of 0.20 d^{-1}, Sherr et al. 2009; and 0.19 d^{-1}, Sherr et al. 2013 for growth rates measured between April and June), but within the range of values reported for polar regions (Schmoker et al. 2013). Phytoplankton growth rates appeared not to be limited by macronutrients on the shelf during our study, as nutrient amendments did not significantly increase phytoplankton growth rates in the majority of experiments (see Table S3 in the Supplement). F_v/F_m values were also indicative of a healthy phytoplankton assemblage (Table S1) (Suggett et al.

2009), suggesting that light limitation may have been the primary factor controlling phytoplankton growth during the spring–summer transition. We did not detect a correlation between phytoplankton growth and percentage of ice coverage (Table S2), but the percentage of ice coverage extracted from SSM/I satellite images does not take into account several factors that may impact light availability, including the ice thickness and the snow thickness atop the ice.

Massive under-ice phytoplankton blooms have been reported in the Chukchi Sea (Arrigo et al. 2012, 2014), as thin, first-year ice cover and extensive melt pond formation both allowed greater light penetration into the water column. This phenomenon has been detected annually in the satellite record from 1998 to 2012 (Lowry et al. 2014). A late season snowfall during the present study delayed the formation of melt ponds and the establishment of under-ice blooms, in agreement with previous results (Fortier et al. 2002) (see Fig. S1). However, continual decreases in ice thickness and extent are anticipated to increase light availability for phytoplankton in the future Arctic Ocean. This may result in higher annual primary productivity in the region, with a greater proportion of ice-free areas that support high area-normalized carbon fixation rates (Brown & Arrigo 2013), as well as more thin, melt-pond covered ice that would foster under-ice blooms (Arrigo et al. 2014).

The highest chl *a* concentration reported in this study (3.49 µg l^{-1}) was in a marginal ice zone (Stn 132; 52% ice coverage) near Point Lay, Alaska. High chl *a* and diatom abundances have been reported previously near Point Lay in May and June 2002 (Sukhanova et al. 2009), as coastal regions along the eastern border of the Chukchi Sea tend to experience early season ice melt due to the heat content of the Alaska Coastal Current (Wood et al. 2015). Negative phytoplankton growth rates (–0.06 d^{-1}) coupled with positive phytoplankton mortality rates (0.19 d^{-1}) as well as nitrate drawdown at Stn 132 (Table 1, Fig. 2) suggested we were measuring the phytoplankton population during its decline.

Phytoplankton growth rates were significantly higher than bacterial growth rates during the spring–summer transition on the Chukchi Shelf (means of 0.47 and 0.06 d^{-1}, respectively). Bacterial abundances were in good agreement with previous reports in Arctic regions (mean = 5.8×10^5 cells ml^{-1}) (Garneau et al. 2008, Terrado et al. 2008, Ortega-Retuerta et al. 2014), as were bacterial production rates (range = 0.10 to 1.38 µg C l^{-1} d^{-1}; Table 2) and bacterial growth rates (range = 0.01 to 0.12 d^{-1}) (Kirchman et al. 2005, 2009a,b, Garneau et al. 2008, Ortega-Retuerta et al. 2014). Low bacterial growth rates during the spring–summer transition ostensibly resulted from low environmental temperatures, which have been shown to limit bacterial production in polar regions compared to temperate or subtropical regions (Kirchman et al. 2009b). Limited phytoplankton production and riverine input at this time of year may also have restricted the availability of labile organic matter for bacterial growth. A significant positive relationship between bacterial production rate and chl *a* concentration, and significant negative relationship between bacterial production rate and the distance of the station from shore, support the contention that dissolved organic matter limited bacterial growth rates during our study, as was observed for under-ice Arctic microbial communities during spring by Niemi et al. (2014).

Phototrophic picoeukaryotes were a minor component of the phytoplankton community in our study, making meager contributions to total photosynthetic biomass (mean = 2.9%; Fig. 3). To our knowledge, this is the first early season (May–June) assessment of phototrophic picoeukaryote growth and mortality rates in the Chukchi Sea. The mean phototrophic picoeukaryote intrinsic growth rate at this time of year (0.28 d^{-1}; Table 1) was similar to those reported for other Western Arctic Regions (0.22 and 0.24 d^{-1}) (Liu et al. 2002, Strom & Fredrickson 2008) and during summer on the Chukchi Shelf (0.39 d^{-1}) (Yang et al. 2014).

Phytoplankton mortality rates were substantial, albeit spatially variable during this study (mean = 0.25 d^{-1}; range = non-significant to 0.73 d^{-1}; Table 1), and generally greater than bacterial mortality rates (mean = 0.03 d^{-1}; range = 0.01 to 0.11). Published phytoplankton mortality rates for the spring–summer transition in the Chukchi Sea (mean = 0.07 d^{-1}, Sherr et al. 2009) and Bering Sea (mean = 0.09 d^{-1}, Sherr et al. 2013) are lower than those reported in the present study. However, our mean mortality rate (0.25 d^{-1}) is less than average mortality rates reported for temperate-to-tropical ecosystems (Calbet & Landry 2004, Schmoker et al. 2013), as might be expected due to low water temperatures during our study. On average, protistan grazers consumed a sizeable fraction (mean = 46%) of daily phytoplankton production (Table 1), in relative agreement with the median value of 57% of reported for polar arctic regions (Schmoker et al. 2013).

Relatively few studies have quantified bacterial mortality in polar regions. Vaqué et al. (2008) measured a rate of removal of bacterial carbon of 0.29 µg C l^{-1} d^{-1} in Franklin Bay, Northwest Territories, Canada,

during spring, on the same order as the mean reported in this study (0.31 µg C l^{-1} d^{-1}; Table 2). Sanders & Gast (2012) measured low rates in the Beaufort Sea and Canada Basin, where bacterivory removed an average of <5% of the bacterial standing stock per day. Our daily average removal rate was also a minor component of the standing stocks of bacterial carbon present in the water (standing stocks ranged from 2.68 to 16.3 µg C l^{-1}). Thus, it appears that bacterial mortality rates are depressed in polar regions relative to lower latitudes during the spring–summer transition, where bacterial standing stock removal is often ~30% d^{-1} (Marrasé et al. 1992, Fuhrman & Noble 1995, Boras et al. 2009, Connell et al. 2017). Nonetheless, bacterial grazer-mediated mortality was in relative balance with bacterial production at 6 of 10 stations in the present study (Fig. 5b, Table 2). Production was substantially higher at 4 of the stations, resulting in averaged bacterial production values exceeding grazing losses (Table 2).

Phytoplankton were the dominant carbon source for protistan grazers in the Bering Strait and Chukchi Sea during our study (Fig. 6). Diatoms persistently dominated the phytoplankton assemblage, as evidenced by their contribution to community biomass (Fig. 3) and chl *a* in the larger size-fractions (Fig. 4). The dominance of diatoms on the Chukchi Shelf is well known (Sherr et al. 2009, Sukhanova et al. 2009, Laney & Sosik 2014, Yang et al. 2014) and presumably reflects the influx of nutrient-replete waters through the Bering Strait (Fig. 2) (Weingartner et al. 2005). The large contribution of phytoplankton carbon to the overall diet of protistan grazers was due to a combination of higher phytoplankton biomass (Fig. 3) combined with higher phytoplankton mortality rates than bacterial mortality rates (Tables 1 & 2).

Although phytoplankton clearly dominated the carbon source for protistan grazers in the present study, it is likely that bacterial carbon contributes a greater percentage of total carbon consumed by protistan grazers as the season progresses into summer. Dilution experiment data compiled for the Western Arctic Ocean indicate that the mean monthly phytoplankton intrinsic growth rate does not change significantly from spring (April μ_0 mean = 0.20 ± 0.14 d^{-1}) to midsummer (June μ_0 mean = 0.25 ± 0.20 d^{-1}) to late summer (August μ_0 mean = 0.22 ± 0.16 d^{-1}) (Sherr et al. 2009, 2013, Yang et al. 2014, present study). A relatively constant mean phytoplankton intrinsic growth rate may reflect a relatively quick transition from a light-limiting environment for phytoplankton in the spring to a nutrient-limiting environment in the summer. In contrast, Kirchman et al. (2009a) observed that bacterial production rates were 3-fold greater during the summer than during the spring in the Chukchi Sea. Increased bacterial production rates in the summer, coupled with relatively constant phytoplankton growth rates, would result in bacterial prey carbon contributing a larger proportion of consumer diet in the summer season.

Microzooplankton dominated phytoplankton and bacterial mortality during the present study. Differences among dilution experiment treatments that included or excluded mesozooplankton did not indicate significant grazing activity by mesozooplankton (see Table S3). Additionally, ciliates were the only grazer assemblage whose biomass was significantly correlated with diatom biomass (the dominant phytoplankton group at most stations). Heterotrophic dinoflagellates are generally considered to be the principal protistan consumer of diatoms (Sherr & Sherr 2007); however, Sherr et al. (2013, and references therein) have reported episodic importance of large ciliates as grazers on diatom genera in both polar and temperate seas. It is possible that ciliates were consuming diatoms during our study, potentially grazing down single-cells and leaving behind the large diatom chains that were observed. It is also possible that dinoflagellates may have been the primary grazers of diatoms in the study, but their abundances were lower than those of ciliates as a result of preferential grazing by mesozooplankton on the dinoflagellates (Levinsen et al. 2000, Campbell et al. 2009, Saiz et al. 2013).

This study, to our knowledge, presents the first direct comparison of phytoplankton and bacterial carbon consumption in a marine polar ecosystem. Phytoplankton, particularly diatoms, were the primary source of prey carbon for higher trophic levels during the spring–summer transition on the Chukchi Sea Shelf. Bacterial contributions to higher trophic levels were small during our study (<1 µg C l^{-1} d^{-1}). An understanding of the relative importance of these processes is fundamental to our assessments of carbon available to higher trophic levels or export out of the euphotic zone. The prevalence of the grazer-based food web in the Arctic provides the energy necessary to foster a wide variety of invertebrates, fish, seabirds, and marine mammals (Grebmeier 2012). Nonetheless, species size and composition may shift as a consequence of climate change. For example, phytoplankton cell size decreased in the Canada basin in response to increased seawater temperatures, freshwater input, and stratification (Li et al. 2009). Our study provides a baseline for Chukchi Sea food web dynamics, which may experience similar shifts in food web structure in the coming years.

Acknowledgements. This research was supported by the National Science Foundation (grant number PLR-1304563 to K.R.A.), a Research Enhancement Fellowship from the University of Southern California to P.E.C., grants from the Natural Sciences and Engineering Research Council of Canada (NSERC) to C.M. (Discovery Grant) and G.M. (Visiting Fellowship in Canadian Laboratory Program), as well as Fisheries and Oceans Canada (International Governance Strategy). We would like to thank the captain and crew of the US Coast Guard 'Healy' for enabling this scientific endeavor. We are grateful to Dan and Laura Schuller (SCRIPPS) for collecting and providing the nutrient data, and Kate Lowry and Gert van Dijken (Stanford) for extracting and providing the satellite-derived sea ice concentrations and satellite imagery. In addition, we are indebted to Hannah Joy-Warren and Caroline Ferguson (Stanford) for operating the fast repetition rate fluorometer (FRRf) and to Andrea Niemi (Fisheries and Oceans Canada) for help with planning and mobilization for the expedition. Finally, we would like to thank other members of the SUBICE science party who consistently offered their assistance in times of need.

LITERATURE CITED

Arar EJ, Collins GB (1997) Method 445.0: *in vitro* determination of chlorophyll *a* and pheophytin *a* in marine and freshwater algae by fluorescence. US Environmental Protection Agency, Washington, DC

Arrigo KR (2015) Impacts of climate on ecosystems and chemistry of the Arctic Pacific environment (ICESCAPE). Deep-Sea Res II 118:1–6

Arrigo KR, van Dijken GL (2015) Continued increases in Arctic Ocean primary production. Prog Oceanogr 136: 60–70

Arrigo KR, Perovich DK, Pickart RS, Brown ZW and others (2012) Massive phytoplankton blooms under Arctic sea ice. Science 336:1408

Arrigo KR, Perovich DK, Pickart RS, Brown ZW and others (2014) Phytoplankton blooms beneath the sea ice in the Chukchi Sea. Deep-Sea Res II 105:1–16

Behrenfeld MJ, Boss ES (2014) Resurrecting the ecological underpinnings of ocean plankton blooms. Annu Rev Mar Sci 6:167–194

Boras JA, Sala MM, Vázquez-Domínguez E, Weinbauer MG, Vaqué D (2009) Annual changes of bacterial mortality due to viruses and protists in an oligotrophic coastal environment (NW Mediterranean). Environ Microbiol 11:1181–1193

Brown ZW, Arrigo KR (2013) Sea ice impacts on spring bloom dynamics and net primary production in the Eastern Bering Sea. J Geophys Res Oceans 118:43–62

Calbet A, Landry MR (2004) Phytoplankton growth, microzooplankton grazing, and carbon cycling in marine systems. Limnol Oceanogr 49:51–57

Campbell RG, Sherr EB, Ashjian CJ, Plourde S, Sherr BF, Hill V, Stockwell DA (2009) Mesozooplankton prey preference and grazing impact in the western Arctic Ocean. Deep-Sea Res II 56:1274–1289

Connell PE, Campbell V, Gellene AG, Hu SK, Caron DA (2017) Planktonic food web structure at a coastal time-series site: II. Spatiotemporal variability of microbial trophic activities. Deep-Sea Res I 121:210–223

Cottrell MT, Kirchman DL (2009) Photoheterotrophic microbes in the Arctic Ocean in summer and winter. Appl Environ Microbiol 75:4958–4966

del Giorgio PA, Bird DF, Prairie YT, Planas D (1996) Flow cytometric determination of bacterial abundance in lake plankton with the green nucleic acid stain SYTO 13. Limnol Oceanogr 41:783–789

Dickinson I, Walker G, Pearce DA (2016) Microbes and the Arctic Ocean. In: Hurst JC (ed) Their world: a diversity of microbial environments. Springer International Publishing, Cham, p 341–381

Fortier M, Fortier L, Michel C, Legendre L (2002) Climatic and biological forcing of the vertical flux of biogenic particles under seasonal Arctic sea ice. Mar Ecol Prog Ser 225:1–16

Franzè G, Lavrentyev PJ (2014) Microzooplankton growth rates examined across a temperature gradient in the Barents Sea. PLOS ONE 9:e86429

Franzè G, Lavrentyev PJ (2017) Microbial food web structure and dynamics across a natural temperature gradient in a productive polar shelf system. Mar Ecol Prog Ser 569:89–102

Fuhrman JA, Noble RT (1995) Viruses and protists cause similar bacterial mortality in coastal seawater. Limnol Oceanogr 40:1236–1242

Gallegos CL (1989) Microzooplankton grazing on phytoplankton in the Rhode River, Maryland: nonlinear feeding kinetics. Mar Ecol Prog Ser 57:23–33

Garneau MÈ, Vincent WF, Alonso-Sáez L, Gratton Y, Lovejoy C (2006) Prokaryotic community structure and heterotrophic production in a river-influenced coastal arctic ecosystem. Aquat Microb Ecol 42:27–40

Garneau MÈ, Roy S, Lovejoy C, Gratton Y, Vincent WF (2008) Seasonal dynamics of bacterial biomass and production in a coastal arctic ecosystem: Franklin Bay, western Canadian Arctic. J Geophys Res Oceans 113: C07S91

Grebmeier JM (2012) Shifting patterns of life in the Pacific Arctic and Sub-Arctic seas. Annu Rev Mar Sci 4:63–78

Holm-Hansen O, Lorenzen CJ, Holmes RW, Strickland JDH (1965) Fluorometric determination of chlorophyll. ICES J Mar Sci 30:3–15

Kirchman DL, Malmstrom RR, Cottrell MT (2005) Control of bacterial growth by temperature and organic matter in the Western Arctic. Deep-Sea Res II 52:3386–3395

Kirchman DL, Hill V, Cottrell MT, Gradinger R, Malmstrom RR, Parker A (2009a) Standing stocks, production, and respiration of phytoplankton and heterotrophic bacteria in the western Arctic Ocean. Deep-Sea Res II 56: 1237–1248

Kirchman DL, Morán XAG, Ducklow H (2009b) Microbial growth in the polar oceans — role of temperature and potential impact of climate change. Nat Rev Microbiol 7: 451–459

Kolber ZS, Prášil O, Falkowski PG (1998) Measurements of variable chlorophyll fluorescence using fast repetition rate techniques: defining methodology and experimental protocols. Biochim Biophys Acta Bioenerg 1367:88–106

Landry MR, Hassett RP (1982) Estimating the grazing impact of marine micro-zooplankton. Mar Biol 67:283–288

Landry RM, Kirshtein J, Constantinou J (1995) A refined dilution technique for measuring the community grazing impact of microzooplankton, with experimental tests in the central equatorial Pacific. Mar Ecol Prog Ser 120: 53–63

Laney SR, Sosik HM (2014) Phytoplankton assemblage structure in and around a massive under-ice bloom in the Chukchi Sea. Deep-Sea Res II 105:30–41

Levinsen H, Turner JT, Nielsen TG, Hansen BW (2000) On the trophic coupling between protists and copepods in arctic marine ecosystems. Mar Ecol Prog Ser 204:65–77

Li WKW, McLaughlin FA, Lovejoy C, Carmack EC (2009) Smallest algae thrive as the Arctic Ocean freshens. Science 326:539

Liu H, Suzuki K, Saino T (2002) Phytoplankton growth and microzooplankton grazing in the subarctic Pacific Ocean and the Bering Sea during summer 1999. Deep-Sea Res I 49:363–375

Lowry KE, van Dijken GL, Arrigo KR (2014) Evidence of under-ice phytoplankton blooms in the Chukchi Sea from 1998 to 2012. Deep-Sea Res II 105:105–117

Marrasé C, Lim EL, Caron DA (1992) Seasonal and daily changes in bacterivory in a coastal plankton community. Mar Ecol Prog Ser 82:281–289

Niemi A, Meisterhans G, Michel C (2014) Response of under-ice prokaryotes to experimental sea-ice DOM enrichment. Aquat Microb Ecol 73:17–28

Olson MB, Strom SL (2002) Phytoplankton growth, microzooplankton herbivory and community structure in the southeast Bering Sea: insight into the formation and temporal persistence of an *Emiliania huxleyi* bloom. Deep-Sea Res II 49:5969–5990

Ortega-Retuerta E, Jeffrey WH, Babin M, Bélanger S and others (2012) Carbon fluxes in the Canadian Arctic: patterns and drivers of bacterial abundance, production and respiration on the Beaufort Sea margin. Biogeosciences 9:3679–3692

Ortega-Retuerta E, Fichot CG, Arrigo KR, Van Dijken GL, Joux F (2014) Response of marine bacterioplankton to a massive under-ice phytoplankton bloom in the Chukchi Sea (Western Arctic Ocean). Deep-Sea Res II 105:74–84

Pearce I, Davidson AT, Thomson PG, Wright S and others (2010) Marine microbial ecology off East Antarctica (30–80° E): rates of bacterial and phytoplankton growth and grazing by heterotrophic protists. Deep-Sea Res II 57: 849–862

Putland JN (2000) Microzooplankton herbivory and bacterivory in Newfoundland coastal waters during spring, summer and winter. J Plankton Res 22:253–277

Rose JM, Caron DA (2007) Does low temperature constrain the growth rates of heterotrophic protists? Evidence and implications for algal blooms in cold waters. Limnol Oceanogr 52:886–895

Saiz E, Calbet A, Isari S, Antó M and others (2013) Zooplankton distribution and feeding in the Arctic Ocean during a *Phaeocystis pouchetii* bloom. Deep-Sea Res I 72:17–33

Sanders RW, Gast RJ (2012) Bacterivory by phototrophic picoplankton and nanoplankton in Arctic waters. FEMS Microbiol Ecol 82:242–253

Schmoker C, Hernández-León S, Calbet A (2013) Microzooplankton grazing in the oceans: impacts, data variability, knowledge gaps and future directions. J Plankton Res 35:691–706

Sherr EB, Sherr BF (1994) Bacterivory and herbivory: key roles of phagotrophic protists in pelagic food webs. Microb Ecol 28:223–235

Sherr EB, Sherr BF (2002) Significance of predation by protists in aquatic microbial food webs. Antonie van Leeuwenhoek 81:293–308

Sherr EB, Sherr BF (2007) Heterotrophic dinoflagellates: a significant component of microzooplankton biomass and major grazers of diatoms in the sea. Mar Ecol Prog Ser 352:187–197

Sherr EB, Sherr BF, Hartz AJ (2009) Microzooplankton grazing impact in the Western Arctic Ocean. Deep-Sea Res II 56:1264–1273

Sherr EB, Sherr BF, Ross C (2013) Microzooplankton grazing impact in the Bering Sea during spring sea ice conditions. Deep-Sea Res II 94:57–67

Smith DC, Azam F (1992) A simple, economical method for measuring bacterial protein synthesis rates in seawater using ^{3}H-leucine. Mar Microb Food Webs 6:107–114

Springer AM, McRoy CP (1993) The paradox of pelagic food webs in the northern Bering Sea — III. Patterns of primary production. Cont Shelf Res 13:575–599

Strom SL, Fredrickson KA (2008) Intense stratification leads to phytoplankton nutrient limitation and reduced microzooplankton grazing in the southeastern Bering Sea. Deep-Sea Res II 55:1761–1774

Suggett DJ, Moore CM, Hickman AE, Geider RJ (2009) Interpretation of fast repetition rate (FRR) fluorescence: signatures of phytoplankton community structure versus physiological state. Mar Ecol Prog Ser 376:1–19

Sukhanova IN, Flint MV, Pautova LA, Stockwell DA, Grebmeier JM, Sergeeva VM (2009) Phytoplankton of the western Arctic in the spring and summer of 2002: structure and seasonal changes. Deep-Sea Res II 56: 1223–1236

Taylor FJR, Hoppenrath M, Saldarriaga JF (2008) Dinoflagellate diversity and distribution. Biodivers Conserv 17: 407–418

Terrado R, Lovejoy C, Massana R, Vincent WF (2008) Microbial food web responses to light and nutrients beneath the coastal Arctic Ocean sea ice during the winter–spring transition. J Mar Syst 74:964–977

Utermöhl H (1958) Zur Gewässertypenfrage tropischer Seen. Verh Int Ver Limnol 13:236–251

Vaqué D, Guadayol O, Peters F, Felipe J and others (2008) Seasonal changes in planktonic bacterivory rates under the ice covered coastal Arctic Ocean. Limnol Oceanogr 53:2427–2438

Weingartner T, Aagaard K, Woodgate R, Danielson S, Sasaki Y, Cavalieri D (2005) Circulation on the north central Chukchi Sea shelf. Deep-Sea Res II 52:3150–3174

Wells LE, Deming JW (2003) Abundance of Bacteria, the Cytophaga-Flavobacterium cluster and Archaea in cold oligotrophic waters and nepheloid layers of the Northwest Passage, Canadian Archipelago. Aquat Microb Ecol 31:19–31

Wood KR, Bond NA, Danielson SL, Overland JE, Salo SA, Stabeno PJ, Whitefield J (2015) A decade of environmental change in the Pacific Arctic region. Prog Oceanogr 136:12–31

Yang EJ, Ha HK, Kang SH (2014) Microzooplankton community structure and grazing impact on major phytoplankton in the Chukchi sea and the western Canada basin, Arctic ocean. Deep-Sea Res II 120:91–102

Editorial responsibility: Ronald Kiene, Mobile, Alabama, USA

Submitted: April 27, 2017; Accepted: July 9, 2018
Proofs received from author(s): August 15, 2018